

PROMO: Promptable Outfitting for Efficient High-Fidelity Virtual Try-On

Haohua Chen^{1,2,*} Tianze Zhou^{1,3,*} Wei Zhu¹ Runqi Wang¹ Yandong Guan^{1,2}
 Dejia Song¹ Yibo Chen¹ Xu Tang¹ Yao Hu¹ Lu Sheng^{2,†} Zhiyong Wu^{3,‡}
¹Xiaohongshu Inc. ²Beihang University ³Tsinghua University



Figure 1. PROMO enables multi-garment try-on, prompt-based control over dressing styles and demonstrates robust performance in challenging real-world scenarios.

Abstract

Virtual Try-on (VTON) has become a core capability for online retail, where realistic try-on results provide reliable fit guidance, reduce returns, and benefit both consumers and merchants. Diffusion-based VTON methods achieve photo-realistic synthesis, yet often rely on intricate architectures such as auxiliary reference networks and suffer from slow sampling, making the trade-off between fidelity and efficiency a persistent challenge. We approach VTON as a structured image editing problem that demands strong conditional generation under three key requirements: subject preservation, faithful texture transfer, and seamless harmonization. Under this perspective, our training framework is generic and transfers to broader image editing tasks. Moreover, the paired data produced by VTON constitutes a rich supervisory resource for training general-purpose editors. We present *PROMO*, a promptable virtual try-on framework built upon a Flow Matching DiT backbone with latent multi-modal conditional concatenation. By leverag-

ing conditioning efficiency and self-reference mechanisms, our approach substantially reduces inference overhead. On standard benchmarks, *PROMO* surpasses both prior VTON methods and general image editing models in visual fidelity while delivering a competitive balance between quality and speed. These results demonstrate that flow-matching transformers, coupled with latent multi-modal conditioning and self-reference acceleration, offer an effective and training-efficient solution for high-quality virtual try-on.

1. Introduction

Virtual Try-on (VTON) aims to render a target garment onto a given person image with high fidelity and realism. It is of practical importance in e-commerce, where it enables shoppers to obtain reliable fit and appearance references without in-store trials, provides interactive experiences, and reduces return rates, benefiting both consumers and merchants.

Early VTON systems predominantly relied on warping-based pipelines [13, 52]. These approaches often yield unnatural appearances and degrade under challenging poses, occlusions, and large non-rigid deformations.

GAN methods [16, 25, 26, 46, 48], improve realism to

* Equal contribution.

† Corresponding author: lsheng@buaa.edu.cn.

‡ Corresponding author: zyw@sz.tsinghua.edu.cn

some extent, yet they commonly struggle to preserve fine garment details and textures, produce coherent shading and illumination, and maintain natural human geometry and articulation.

Spurred by the superior image synthesis performance of diffusion models [15, 32, 34], a growing body of VTON research leverages diffusion-based generative modeling [5–7, 9, 11, 19, 22, 29, 37, 47], demonstrating clear gains in visual fidelity and controllability. Many approaches use a diffusion UNet [35] or Transformer model [42], adding conditions by using a reference net to create condition tokens, which are then appended to the main denoising net’s key/query sequences. These methods [5, 19, 37, 47], require another whole net, resulting in complex initialization and interaction logic between the two nets. Other approaches [6, 31] use image-level concatenation (e.g., concatenating condition images as a larger image) to inject conditions. However, considering information density, parts of the conditions do not need to be at the same resolution as the output images.

Moreover, the dressing style of the garment varies. Some works overlook this, replacing the text encoder with an image encoder. PromptDresser [22] uses prompts to control dressing style, but it requires a closed-source VLM to caption the dressing style.

In summary, the contributions of this work include:

- We propose PROMO, a multi-modal, prompt-controllable (promptable) virtual try-on framework. Leveraging a temporal self-reference mechanism across denoise timesteps, group-wise attention mask modulation, and efficient token merging, PROMO attains fast yet high-quality generation with a large-parameter Diffusion Transformer (DiT) backbone.
- Motivated by real-world virtual try-on applications, we propose a Style Prompt System by tuning Qwen2.5-VL-7B, which provides reliable style description to support promptable control and downstream evaluation.
- We conduct extensive experiments on the public VITON-HD and DressCode datasets and demonstrate consistent gains over state-of-the-art baselines VTON models and image-editing model in benchmark, achieving superior visual quality and realism.

2. Related Work

2.1. Image-based Virtual Try-on

Image-based virtual try-on synthesizes realistic images of a person wearing a target garment. Early warping-based methods used a two-stage pipeline (warping and fusion) with techniques like Thin Plate Spline (TPS) [48, 53] or appearance flow [13], but suffered from alignment artifacts.

Diffusion-based approaches now dominate, avoiding ex-

plicit warping. LaDI-VTON [29] and StableVITON [21] use ControlNet [50]-inspired conditioning. Others, like OOTDiffusion [47], IMAGDressing-v1 [38] and IDM-VTON [5], employ parallel “reference nets” to encode garment features.

Recent works like PromptDresser [22] leverages LMMs for text-editable style control (e.g. “tuck”, “fit”) via prompt-aware masks to enhance controllability. Any2AnyTryon [11] uses a unified, mask-free DiT framework for multiple tasks, like layered try-on and garment reconstruction, using adaptive position embeddings to handle variable inputs.

Existing diffusion methods often require complex architectures, motivating our pursuit of a more efficient framework.

2.2. Diffusion Models

U-Net [35] was the predominant backbone for diffusion models like LDM [34] and SDXL [33]. DiT [32] successfully replaced the U-Net with a Transformer, demonstrating strong scalability. Recent models like Stable Diffusion 3 [8] and FLUX [23, 24] build on this, using transformer blocks and flow-matching formulations to predict velocity fields. We leverage the Diffusion Transformer architecture for its scalability, making it an ideal backbone for high-quality virtual try-on and capturing fine-grained garment details.

2.3. Multi-Condition Image Generation

Virtual try-on is essentially a multi-conditional portrait generation task, closely related to multi-condition image generation models. FLUX-Kontext [24] extends FLUX [24] to support text-plus-single-image conditioning, but struggles when handling multiple reference images. DreamO [30] injects conditions via learnable embeddings, which suffer from limited generalization. UNO [45] proposes a model-data co-evolution paradigm that leverages Text-to-Image (T2I) models to generate high-quality single-subject data, thereby training stronger Subject-to-Image (S2I) models capable of producing diverse multi-subject outputs. Omini-Control [40] separates subject and spatial conditions by toggling 2D positional-encoding offsets, implicitly assuming one reference per condition type, an assumption that fails in try-on scenarios with multiple garments. IC-LoRA [18] concatenates images at pixel level, ignoring heterogeneous information density across conditions and either sacrificing resolution or increasing computational cost.

3. Method

3.1. Overview

3.1.1. Modeling

The overall framework of PROMO is shown in Fig. 2. Given a person image I_P , garment images I_{G_i} and optional

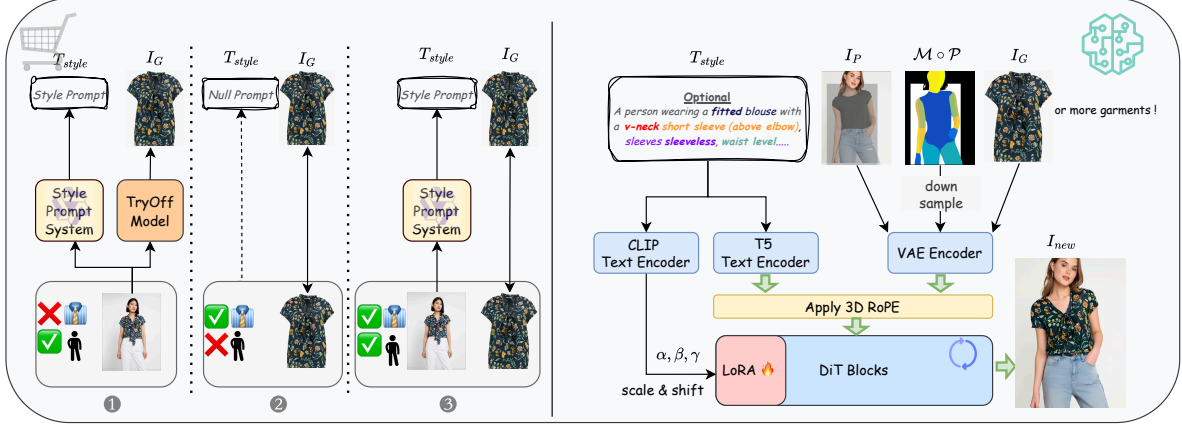


Figure 2. Overview of scenarios handled by our PROMO framework. The left panel illustrates three common scenarios that customers encounter during online shopping: 1) model image available without a specific garment image, 2) garment image available without a model, and 3) both model and garment images available. Our system addresses the missing information in each scenario by generating the necessary conditional inputs required by our model. Notably, for scenarios without model images, our system features pure image-reference capability, allowing text prompts to be omitted while maintaining a robust baseline performance.

clothing style description T_{style} extracted by Style Prompt System from I_{model} . Our model aims to generate an image I_{new} , where the person wears the given garments in the specified dressing style. It can be formulated as:

$$I_{new} = \mathcal{F}(I_p, \{I_{G_i}\}_{i=1}^N, T_{style}^*) \quad (1)$$

$$\mathcal{C} = \{\mathcal{E}(\tilde{I}_p), \{\mathcal{E}(I_{G_i})\}_{i=1}^N, \mathcal{E}(\mathcal{M} \circ \mathcal{P})\} \quad (2)$$

$$\mathbf{z}_0 = \text{FM}(\mathbf{z}_T, \mathcal{C}, T_{style}^*), \quad \mathbf{z}_T \sim \mathcal{N}(0, \mathbf{I}) \quad (3)$$

$$I_{new} = \mathcal{D}(\mathbf{z}_0) \quad (4)$$

where $\tilde{I}_p = I_p \odot (1 - \mathcal{M})$ is the masked person image, \mathcal{E} is the unified image encoder, \mathcal{M} and \mathcal{P} denote segmentation masks and pose features with \circ representing the overlay merging operation, $\text{FM}(\cdot)$ represents the flow matching model, \mathcal{D} is the VAE decoder, and $*$ indicates optional input.

3.1.2. System for Real-World Scenarios

Real-world e-commerce scenarios often present incomplete inputs. We address this with two auxiliary modules:

Style Prompt System: Generates textual descriptions T_{style} of dressing styles from garment catalog images using a distilled Qwen VL 7B model (Sec. 3.3).

TryOff Model: When an isolated garment image I_{G_i} is unavailable, we instead use the corresponding human model image I_{model} . We extract the garment via our TryOff module:

$$I_{G_i} = \text{TryOff}(I_{model}, T_{garment})$$

where $T_{garment}$ specifies the target garment region. This enables the system to leverage un-paired data during both training and inference, broadening its applicability.

3.2. Precise and Efficient Spatial Conditioning

3.2.1. Agnostic Mask Generation

Virtual try-on requires erasing clothing at corresponding body regions to prevent information leakage. Unlike traditional masks in datasets like VITON-HD [4] that rely on body parsing with dilation or manual annotation, we adopt the approach from FitDiT [19], combining human body parsing with DWPose [49] for automated mask generation. This method automatically generates upper-body, lower-body, or full-body masks based on the garment type, seamlessly integrating into our generation pipeline.

3.2.2. Precise Body Shape Estimation

Masks remove original clothing information but inevitably lose body shape and pose details. Therefore, extracting human pose and shape is critical for high-fidelity virtual try-on. DensePose [12] estimates body parts, pose, and shape, but produces distorted results on loose-fitting garments like long skirts, causing information leakage and poor inference. DWPose [49] extracts only pose information without shape. However, lacking body shape data, pose-only models fail to handle different body types accurately. To address this, we leverage EOMT [20] and employ an iterative image generation training to develop a more accurate pose and shape estimation model that is robust to clothing occlusion. Fig. 3 shows the comparison of ours and original DensePose.

3.2.3. Spatial Condition Merging

While IC-LoRA [18] and CatVTON [6] attempt to inject image conditions via image-level concatenation, this approach necessitates uniform resolution across all concatenated images. In our virtual try-on pipeline, the person image resolution is 1024×768 , whereas the mask and pose conditions contain substantial information redundancy and



Figure 3. Compared to directly using the original DensePose [12], our method better estimates plausible body shapes under loose clothing, effectively preventing information leakage.

In preprocessing (from pixel resolution to latent resolution)

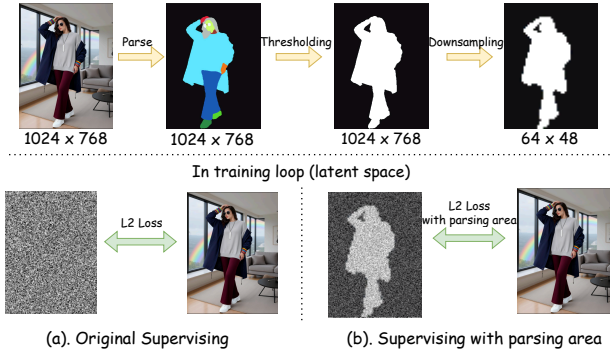


Figure 4. We downsample the extracted human parsing to match the resolution of the latent space. Compared to the standard supervision in (a), we adopt a weighted loss design in (b).

do not require such high fidelity.

Inspired by OminiControl2 [41], we apply 2x downsampling along height and width to the mask and pose conditions in pixel space, thereby reducing their token count to 25% in latent space.

We further merge the pose condition onto the mask condition. As shown in Fig. 5, this hierarchical compression reduces the final token count to merely 12.5% of the original dual-condition representation, resulting in improvements in both training and inference efficiency.

3.2.4. Region-Aware Loss Weighting

In virtual try-on tasks, models often face a trade-off between reconstructing backgrounds and garment textures, where excessive focus on backgrounds may distract from clothing details.

We leverage human parsing results to distinguish body and background regions. The parsing mask is downsampled by 16x to match latent space resolution, constructing a region-aware weight map: body regions receive weight $1 + \lambda$, backgrounds receive $1 - \lambda$. This strategy enables

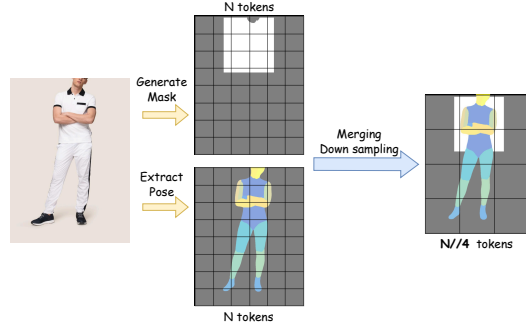


Figure 5. Our method for efficient spatial condition injection. We directly paste the pose condition onto the agnostic image, then perform downsampling, eventually to reduce the 2N tokens to N/4 tokens, achieving 87.5% token reduction.

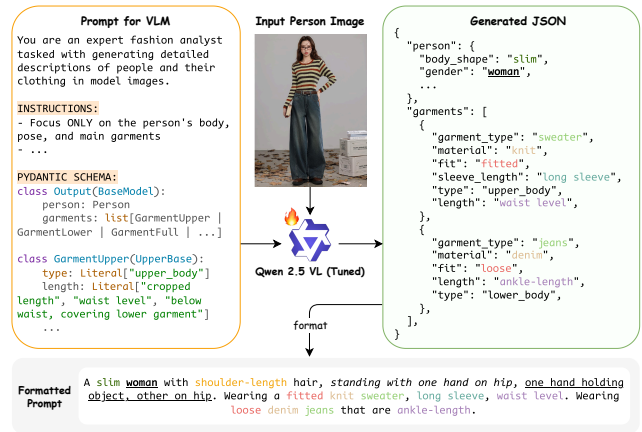


Figure 6. Overview of the Style Prompt System. A finetuned VLM processes an image of a person wearing the source garment, extracting person and garment attributes into a JSON format. This structured JSON is then converted into a natural language prompt for our pipeline.

the model to focus on garment details while reducing background interference.

$$M_{\text{latent}} = \text{Downsample}(M_{\text{parsing}}, s = 16) \quad (5)$$

$$W = M_{\text{latent}} \cdot (1 + \lambda) + (1 - M_{\text{latent}}) \cdot (1 - \lambda) \quad (6)$$

$$\mathcal{L}_{\text{weighted}} = \mathbb{E}_{t, z_0, \epsilon} [\mathbf{W} \odot \|v - v_{\theta}(z_t, t, \mathbf{c})\|^2] \quad (7)$$

where M_{parsing} is the binary parsing mask, W is the weight map, $\lambda \in [0, 1)$ controls weighting intensity, and \odot denotes element-wise multiplication.

3.3. Promptable Dressing Style

Corresponding images of models wearing garments contain valuable information about wearing styles and garment-body spatial relationships. Therefore, unlike FiTDiT [19] that discards text control, we retain the text embedding component.

PromptDresser [22] introduced a prompt extraction pipeline using GPT-4o [1]. However, we identify several

drawbacks: 1) its reliance on few-shot examples leads to substantial token consumption; 2) our inspection revealed numerous extraction inaccuracies; and 3) it is limited to extracting attributes for only a single garment. This last limitation is critical, as describing all other garments is crucial for maintaining outfit consistency.

To address these issues, we designed a new pipeline. First, we created a comprehensive, multi-garment JSON schema and used Pydantic to generate an OpenAPI-compliant specification, which we found LLMs parse more reliably than natural language descriptions. Second, to reduce cost and improve accuracy, our pipeline uses only the single person image as input. We employ a two-stage strategy: a large Qwen2.5-VL-72B [2] model annotates a small dataset, which we then strictly filter to remove all non-compliant annotations. This cleaned dataset is used to fine-tune a much smaller Qwen2.5-VL-7B model. The resulting 7B model is not only significantly faster but also achieves higher accuracy than the 72B model, as it was trained exclusively on valid, schema-compliant data.

3.4. Temporal Self-Reference for Group Conditions

To enable efficient multi-condition integration in FLUX [23], we introduce Temporal Self-Reference, a parameter-free mechanism using 3D-RoPE for scalable condition grouping and injection.

3.4.1. Temporal Self-Reference

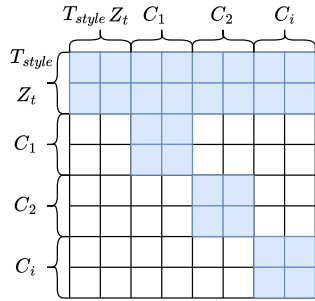


Figure 7. Attention mechanism: z_t and T_{style} have global visibility, while C_i only attends to itself.

Traditional reference networks require doubled parameters [19]. FastFit [7] introduces temporal self-reference on UNet [35] to avoid this. We extend it to diffusion transformers with reduced spatial condition overhead.

As shown in Fig. 7, each C_i self-attends, while T_{style} and z_t have global visibility. At inference (Fig. 8), we cache C_i Key-Value pairs at the first timestep and reuse them with Query containing only T_{style} and z_t :

$$Q = [Q_{z_t}, Q_{T_{style}}] \quad (8)$$

$$K = [K_{z_t}, K_{T_{style}}, K_{C_1}^{\text{cached}}, \dots, K_{C_n}^{\text{cached}}] \quad (9)$$

$$V = [V_{z_t}, V_{T_{style}}, V_{C_1}^{\text{cached}}, V_{C_2}^{\text{cached}}, \dots, V_{C_n}^{\text{cached}}] \quad (10)$$

This achieves nearly lossless quality without reference network duplication.

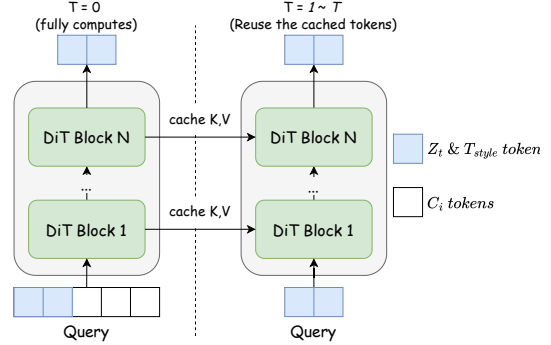


Figure 8. Temporal Self-Reference mechanism.

3.4.2. Group Conditioning by 3D-RoPE

Building upon OminiControl [40] and FLUX Kontext [24], we repurpose RoPE’s [39] temporal dimension as group condition identifiers, distinguishing multiple conditions via position encodings:

$$(t, x, y)_{z_t} = (0, x_{z_t}, y_{z_t}) \quad (11)$$

$$(t, x, y)_{c_i} = \begin{cases} (i, x, y)_{z_t} & \text{for spatial conditions} \\ (i, x, y + \Delta)_{z_t} & \text{for garment conditions} \end{cases} \quad (12)$$

This parameter-free approach enables **single-garment** training and **multi-garment** inference in a **single forward pass**, avoiding iterative error accumulation.

4. Experiment

4.1. Dataset

Our experiments are conducted on two public datasets and one self-collected in-the-wild dataset. VITON-HD [4] comprises 13,679 image pairs of upper-body garments, with 2,032 pairs designated for testing. DressCode [28] contains 53,792 image pairs spanning three categories (upper-body, lower-body, and dresses), including 5,400 pairs reserved for evaluation. For the in-the-wild dataset, we curate 13 human model images and 40 garment images, generating 520 image pairs through exhaustive combinations. For all test datasets, we employ our self-trained DensePose model.

4.2. Implementation Detail

We build our model upon the FLUX.1-dev version [24], employing Low-Rank Adaptation (LoRA) [17] to efficiently fine-tune all linear layers in the Diffusion Transformer component. With a LoRA rank of 128, this introduces 580M trainable parameters. λ for parsing loss is set to 0.5. We adopt the Prodigy [27] optimizer with its default learning rate of 1.

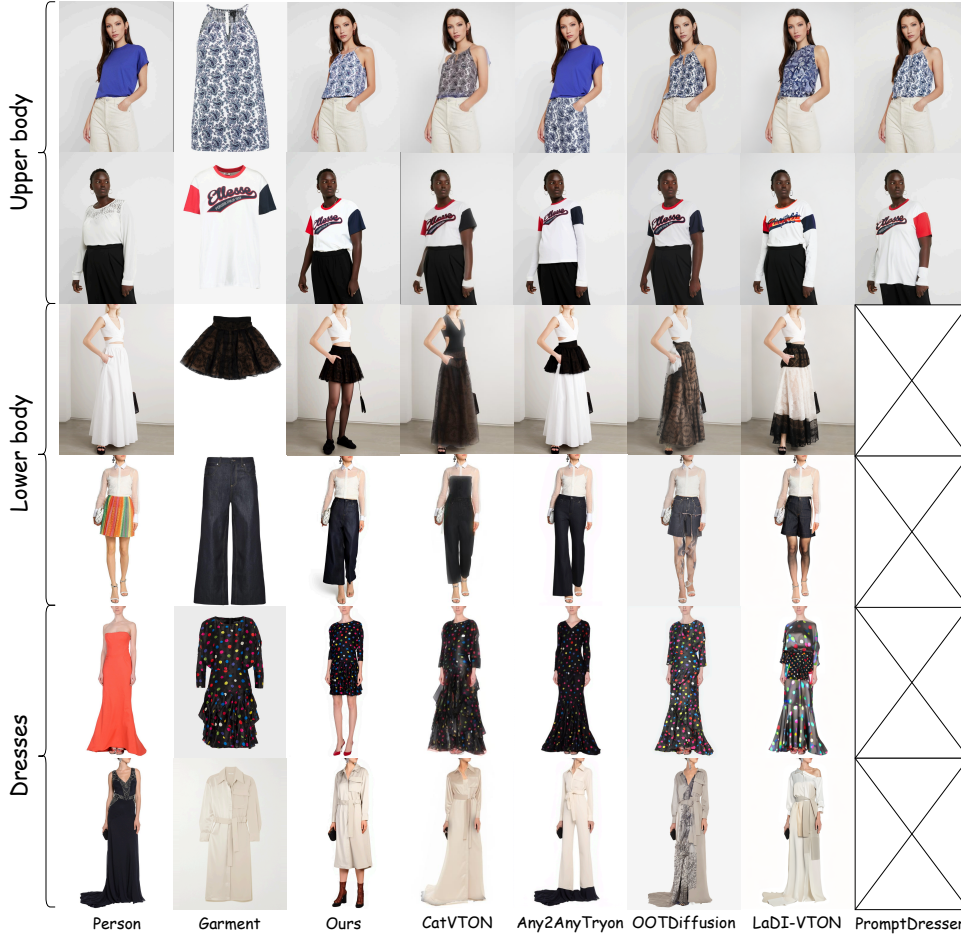


Figure 9. Visualization of comparison between ours and baseline models on DressCode dataset. Best viewed when zoomed in.

All experiments are conducted on the training splits of VITON-HD [4] and DressCode [28] datasets at a resolution of 1024×768. Training is performed on 16 NVIDIA H800 GPUs with an effective batch size of 16 for 90,000 steps.

4.3. Metrics

We evaluate our PROMO by comparing it with prior virtual try-on approaches and image editing models. For the quantitative evaluation on VITON-HD and DressCode datasets, we utilize SSIM [43], LPIPS [51], FID [14], and KID [3] metrics for paired data, while employing FID and KID for unpaired data. Additionally, we conduct subjective evaluations through user studies on in-the-wild datasets, comparing our method against state-of-the-art commercial virtual try-on models.

4.4. Qualitative Comparison

Fig. 9 presents visualization results of virtual try-on on the open-source VITON-HD and DressCode datasets. As shown, other methods exhibit various artifacts, while our approach more completely and naturally transfers garment details onto the person, preserving intricate textures and text

patterns with high fidelity.

Fig. 10 compares our method with general-purpose image editing models, including Seedream 4.0 [36], Qwen Image Edit 2509 [44], and Nanobanana (Gemini 2.5-Flash-Image), on VITON-HD and DressCode datasets. The results demonstrate that general image editing models suffer from color inconsistencies and prominent artifacts in virtual try-on tasks, whereas our model generates more natural and realistic results.

4.5. Quantitative Comparison

4.5.1. On Open-source Dataset

We conduct quantitative experiments on both paired and unpaired subsets of VITON-HD [4] and DressCode [28] datasets. Overall, our model surpasses existing state-of-the-art methods, as demonstrated in Tab. 1.

Tab. 2 presents comparisons with general image editing models mentioned in Sec. 4.4. Due to API rate limitations of closed-source models, we evaluate on a fixed-size subset for this comparison. The results show that our method outperforms image editing models across all metrics.

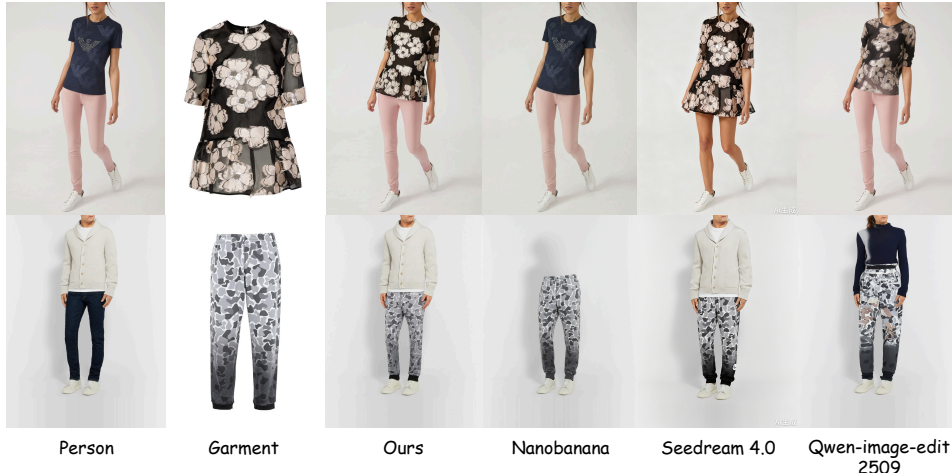


Figure 10. Visualization of comparison on virtual try-on between our PROMO between state-of-the-art image-editing model on DressCode dataset. Best viewed when zoomed in.

Methods	DressCode						VITON-HD					
	Paired			Unpaired			Paired			Unpaired		
	SSIM \uparrow	LPIPS \downarrow	FID \downarrow	KID \downarrow	FID \downarrow	KID \downarrow	SSIM \uparrow	LPIPS \downarrow	FID \downarrow	KID \downarrow	FID \downarrow	KID \downarrow
LaDI-VTON[29]	0.7564	0.3800	5.4700	1.9270	7.3475	2.4690	0.8721	0.1531	6.8500	1.3766	9.6131	<u>2.0207</u>
CatVTON[6]	<u>0.8944</u>	0.1600	6.5372	3.9591	8.4567	4.4897	0.8673	0.1882	9.4412	4.7389	12.5716	5.4555
OOTDiffusion[47]	0.8883	0.0800	3.6623	<u>0.8550</u>	7.0463	2.7910	0.7919	0.1905	32.8944	20.0843	39.9626	26.0686
Any2AnyTryon[11]	0.9107	0.1208	3.0828	1.0565	<u>5.5404</u>	<u>1.5258</u>	<u>0.8705</u>	0.1569	7.1238	2.1797	10.3120	2.7086
PromptDresser[22]	-	-	-	-	-	-	0.8546	<u>0.1163</u>	7.4172	1.5874	10.4356	2.0531
PROMO (Ours)	0.8913	<u>0.0887</u>	<u>3.3103</u>	0.4902	4.7393	0.4992	0.8619	0.1111	<u>6.8903</u>	<u>1.4895</u>	<u>9.9034</u>	1.9174

Table 1. Quantitative results on VITON-HD and DressCode datasets. We compare the metrics under both paired (model’s clothing is the same as the given cloth image) and unpaired settings (model’s clothing differs) with other methods.

Methods	DressCode						VITON-HD					
	Paired			Unpaired			Paired			Unpaired		
	SSIM \uparrow	LPIPS \downarrow	FID \downarrow	KID \downarrow	FID \downarrow	KID \downarrow	SSIM \uparrow	LPIPS \downarrow	FID \downarrow	KID \downarrow	FID \downarrow	KID \downarrow
Qwen-Image-Edit-2509 [44]	0.8370	0.1831	13.5464	1.9944	13.9163	2.7315	0.7790	0.2174	20.6403	0.5018	<u>18.7954</u>	<u>1.1485</u>
Seedream 4.0 [36]	0.8217	0.1816	16.8140	7.2200	25.4943	6.1900	0.7600	0.2352	26.9076	9.3880	26.8181	8.4790
Nanobanana[10]	<u>0.8647</u>	<u>0.1186</u>	<u>10.7050</u>	<u>1.0860</u>	<u>10.6720</u>	<u>0.7160</u>	<u>0.8100</u>	<u>0.1520</u>	<u>19.1688</u>	<u>1.1299</u>	20.4191	0.4411
PROMO (Ours)	0.8919	0.0885	8.9268	0.4674	10.1217	0.5763	0.8439	0.1365	15.6658	2.0513	18.0356	1.5828

Table 2. Quantitative results on VITON-HD and DressCode datasets. Comparison between our model with image-editing methods.

4.5.2. User Study on In-The-Wild Dataset

We conducted a user study comparing our method with three commercial virtual try-on services. The evaluation used 13 person images paired with 40 in-the-wild garment images covering upper-body, lower-body, and dress categories, yielding 520 try-on results. 9 independent annotators assessed each result across four dimensions: (1) garment texture consistency, (2) body shape consistency, (3) garment style consistency, and (4) garment color consistency. A result is considered excellent if more than half of the annotators rate it as such. Tab. 3 reports the excellence rate of each method across all dimensions.

4.6. Ablation Studies

Parsing Area Loss We validate Parsing Area Loss contribution to garment detail preservation through controlled

Method	Texture \uparrow	Body Shape \uparrow	Style \uparrow	Color \uparrow	Overall \uparrow
Huiwa	<u>94.42</u>	88.85	<u>94.80</u>	99.04	<u>78.85</u>
Kling	87.12	<u>93.46</u>	79.87	96.53	60.19
Douyin	96.73	79.04	85.19	95.77	61.54
PROMO (Ours)	93.65	94.62	96.92	<u>97.88</u>	84.42

Table 3. Excellence rates (%) of different methods on in-the-wild dataset. A result is considered excellent if more than half annotators rate it as such. Overall indicates the percentage of images that are excellent in all four dimensions. **Bold** denotes the best result and underline denotes the second best.

ablation experiments comparing two model variants under identical configurations, differing only in this component. As shown in Fig. 12 and Tab. 4, while quantitative improvements on open-source benchmarks are marginal due to their clean backgrounds, qualitative advantages become evident in challenging real-world scenarios. We present represen-

	Paired				Unpaired	
	SSIM \uparrow	LPIPS \downarrow	FID \downarrow	KID \downarrow	FID \downarrow	KID \downarrow
- w/o parsing area loss	<u>0.8896</u>	0.0872	3.2847	<u>0.5076</u>	4.6390	0.9535
- w/o style prompt	<u>0.8896</u>	0.0926	3.7178	0.8926	<u>5.3516</u>	<u>0.6180</u>
- w/o 3D-RoPE	0.8702	0.1304	6.7293	1.7160	7.8175	2.2801
PROMO (Ours)	0.8913	<u>0.0887</u>	<u>3.3103</u>	0.4902	<u>5.3516</u>	0.4992

Table 4. Ablation study on DressCode dataset. The best and second-best results are highlighted in **bold** and underlined, respectively.

tative examples from In-The-Wild datasets featuring complex backgrounds, where the model with Parsing Area Loss achieves notably higher fidelity in reproducing fine-grained garment patterns.



Figure 11. Visualization of ablation study on parsing area loss. Best viewed when zoomed in.

Dressing Style Prompt To investigate the impact of text conditions on virtual try-on performance, we design a controlled experiment: inference on the same test set using both null prompts and descriptive prompts. Although the model supports null prompt try-on generation by design, experimental results demonstrate that appropriate text guidance still yields positive effects. Quantitative comparisons in Tab. 4 indicate that prompt introduction brings marginal improvements in metrics, while also providing users with an optional dimension for style control.

3D-RoPE To demonstrate that 3D-RoPE enhances the model’s capability to distinguish different condition groups and multiple instances within the same category, we conduct ablation experiments by removing positional encodings from all condition tokens while preserving those for text and latent tokens. As shown in Fig. 12 and Tab. 4, the model without 3D-RoPE fails to correctly dress the person with the target garments and produces noticeable artifacts.

Temporal Self-Reference. To validate the effectiveness of the Temporal Self-Reference mechanism in balancing generation quality and inference speed, we conduct comparative experiments on the open-source test set. The experiments compare models with and without this mechanism across generation quality metrics and inference speed. As shown in Tab. 5, Temporal Self-Reference significantly re-

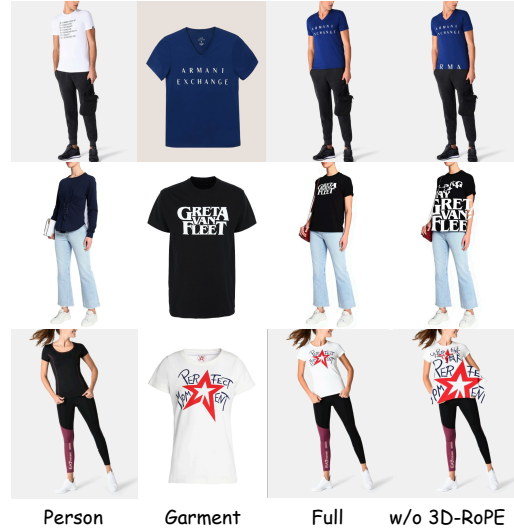


Figure 12. Visualization of ablation study on 3D-RoPE. Without 3D-RoPE, the model fails to correctly distinguish subject transfer and spatial alignment relationships between conditions.

	Inference time (s)	Paired				Unpaired	
		SSIM \uparrow	LPIPS \downarrow	FID \downarrow	KID \downarrow	FID \downarrow	KID \downarrow
- w/o T.S.R	22.2378	<u>0.8913</u>	<u>0.0887</u>	3.3102	0.7975	4.7391	0.5313
- w/o S.T.M	11.1030	0.8916	0.0873	3.4878	<u>0.5126</u>	4.8546	0.4907
PROMO (Ours)	9.1775	<u>0.8913</u>	<u>0.0887</u>	<u>3.3103</u>	0.4902	<u>4.7393</u>	<u>0.4992</u>

Table 5. Quantitative ablation results on DressCode, including quality metrics and inference time. **T.S.R** is for Temporal Self-Reference and **S.T.M** is for Spatial Token Merging. Inference time is averaged over 20 runs on an H800 GPU.

duces inference steps while maintaining generation quality, confirming the effectiveness of this mechanism in the efficiency-quality trade-off.

Spatial Condition Merging. To evaluate the impact of the spatial condition merging strategy, we train a baseline model without condition merging as a control. The comparison of generation speed and quality between the two models on the test set is shown in Tab. 5. Experiments demonstrate that spatial condition merging significantly reduces computational overhead while having negligible impact on generation quality, validating the rationality of exploiting spatial redundancy.

5. Conclusion

We introduced PROMO, a novel virtual try-on framework built on a Flow Matching DiT backbone. By leveraging latent multi-modal conditional concatenation and a temporal self-reference mechanism, our model achieves a superior balance between fidelity and efficiency. PROMO supports multi-garment try-on and prompt-based style control. Experiments on VITON-HD, DressCode, and in-the-wild datasets demonstrate that our method surpasses prior VTON and general image-editing models in both visual quality and inference speed.

References

- [1] Josh Achiam, Steven Adler, Sandhini Agarwal, Lama Ahmad, Ilge Akkaya, Florencia Leoni Aleman, Diogo Almeida, Janko Altenschmidt, Sam Altman, Shyamal Anadkat, et al. Gpt-4 technical report. *arXiv preprint arXiv:2303.08774*, 2023. 4
- [2] Shuai Bai, Keqin Chen, Xuejing Liu, Jialin Wang, Wenbin Ge, Sibao Song, Kai Dang, Peng Wang, Shijie Wang, Jun Tang, Humen Zhong, Yuanzhi Zhu, Mingkun Yang, Zhaohai Li, Jianqiang Wan, Pengfei Wang, Wei Ding, Zheren Fu, Yiheng Xu, Jiabo Ye, Xi Zhang, Tianbao Xie, Zesen Cheng, Hang Zhang, Zhibo Yang, Haiyang Xu, and Junyang Lin. Qwen2.5-vl technical report, 2025. 5
- [3] Mikołaj Bińkowski, Danica J. Sutherland, Michael Arbel, and Arthur Gretton. Demystifying mmd gans, 2021. 6
- [4] Seunghwan Choi, Sunghyun Park, Minsoo Lee, and Jaegul Choo. Viton-hd: High-resolution virtual try-on via misalignment-aware normalization, 2021. 3, 5, 6
- [5] Yisol Choi, Sangkyung Kwak, Kyungmin Lee, Hyungwon Choi, and Jinwoo Shin. Improving diffusion models for authentic virtual try-on in the wild. In *European Conference on Computer Vision*, pages 206–235. Springer, 2024. 2
- [6] Zheng Chong, Xiao Dong, Haoxiang Li, Shiyue Zhang, Wenqing Zhang, Xujie Zhang, Hanqing Zhao, and Xiaodan Liang. Catvton: Concatenation is all you need for virtual try-on with diffusion models, 2024. 2, 3, 7
- [7] Zheng Chong, Yanwei Lei, Shiyue Zhang, Zhuandi He, Zhen Wang, Xujie Zhang, Xiao Dong, Yiling Wu, Dongmei Jiang, and Xiaodan Liang. Fastfit: Accelerating multi-reference virtual try-on via cacheable diffusion models, 2025. 2, 5
- [8] Patrick Esser, Sumith Kulal, Andreas Blattmann, Rahim Entezari, Jonas Müller, Harry Saini, Yam Levi, Dominik Lorenz, Axel Sauer, Frederic Boesel, Dustin Podell, Tim Dockhorn, Zion English, Kyle Lacey, Alex Goodwin, Yanik Marek, and Robin Rombach. Scaling rectified flow transformers for high-resolution image synthesis, 2024. 2
- [9] Hongxing Fan, Zehuan Huang, Lipeng Wang, Haohua Chen, Li Yin, and Lu Sheng. Parts2whole: Generalizable multi-part portrait customization. *IEEE Transactions on Image Processing*, 34:5241–5256, 2025. 2
- [10] Google. Introducing gemini 2.5 flash. <https://developers.googleblog.com/en/introducing-gemini-2-5-flash-image/>, 2024. Accessed: 2025-01-15. 7
- [11] Hailong Guo, Bohan Zeng, Yiren Song, Wentao Zhang, Chuang Zhang, and Jiaming Liu. Any2anytryon: Leveraging adaptive position embeddings for versatile virtual clothing tasks, 2025. 2, 7
- [12] Rıza Alp Güler, Natalia Neverova, and Iasonas Kokkinos. Densepose: Dense human pose estimation in the wild, 2018. 3, 4
- [13] Sen He, Yi-Zhe Song, and Tao Xiang. Style-based global appearance flow for virtual try-on. In *Proceedings of the IEEE/CVF conference on computer vision and pattern recognition*, pages 3470–3479, 2022. 1, 2
- [14] Martin Heusel, Hubert Ramsauer, Thomas Unterthiner, Bernhard Nessler, and Sepp Hochreiter. Gans trained by a two time-scale update rule converge to a local nash equilibrium. *Advances in neural information processing systems*, 30, 2017. 6
- [15] Jonathan Ho, Ajay Jain, and Pieter Abbeel. Denoising diffusion probabilistic models, 2020. 2
- [16] Shion Honda. Viton-gan: Virtual try-on image generator trained with adversarial loss. *Eurographics 2019 - Posters*, 2019. 1
- [17] Edward J. Hu, Yelong Shen, Phillip Wallis, Zeyuan Allen-Zhu, Yuanzhi Li, Shean Wang, Lu Wang, and Weizhu Chen. Lora: Low-rank adaptation of large language models, 2021. 5
- [18] Lianghua Huang, Wei Wang, Zhi-Fan Wu, Yupeng Shi, Huanzhang Dou, Chen Liang, Yutong Feng, Yu Liu, and Jingren Zhou. In-context lora for diffusion transformers, 2024. 2, 3
- [19] Boyuan Jiang, Xiaobin Hu, Donghao Luo, Qingdong He, Chengming Xu, Jinlong Peng, Jiangning Zhang, Chengjie Wang, Yunsheng Wu, and Yanwei Fu. Fitdit: Advancing the authentic garment details for high-fidelity virtual try-on, 2024. 2, 3, 4, 5
- [20] Tommie Kerssies, Niccolò Cavagnero, Alexander Hermans, Narges Norouzi, Giuseppe Averta, Bastian Leibe, Gijs Dubbelman, and Daan de Geus. Your ViT is Secretly an Image Segmentation Model. In *Proceedings of the IEEE/CVF Conference on Computer Vision and Pattern Recognition (CVPR)*, 2025. 3
- [21] Jeongho Kim, Guojung Gu, Minh Park, Sunghyun Park, and Jaegul Choo. Stableviton: Learning semantic correspondence with latent diffusion model for virtual try-on. In *Proceedings of the IEEE/CVF Conference on Computer Vision and Pattern Recognition*, pages 8176–8185, 2024. 2
- [22] Jeongho Kim, Hoyeong Jin, Sunghyun Park, and Jaegul Choo. Promptdresser: Improving the quality and controllability of virtual try-on via generative textual prompt and prompt-aware mask, 2024. 2, 4, 7
- [23] Black Forest Labs. Flux. <https://github.com/black-forest-labs/flux>, 2024. 2, 5
- [24] Black Forest Labs, Stephen Batifol, Andreas Blattmann, Frederic Boesel, Saksham Consul, Cyril Diagne, Tim Dockhorn, Jack English, Zion English, Patrick Esser, Sumith Kulal, Kyle Lacey, Yam Levi, Cheng Li, Dominik Lorenz, Jonas Müller, Dustin Podell, Robin Rombach, Harry Saini, Axel Sauer, and Luke Smith. Flux.1 kontext: Flow matching for in-context image generation and editing in latent space, 2025. 2, 5
- [25] Kathleen M Lewis, Srivatsan Varadarajan, and Ira Kemelmacher-Shlizerman. Tryongan: Body-aware try-on via layered interpolation, 2021. 1
- [26] Yifang Men, Yiming Mao, Yuning Jiang, Wei-Ying Ma, and Zhouhui Lian. Controllable person image synthesis with attribute-decomposed gan. In *Computer Vision and Pattern Recognition (CVPR), 2020 IEEE Conference on*, 2020. 1
- [27] Konstantin Mishchenko and Aaron Defazio. Prodigy: An expeditiously adaptive parameter-free learner, 2024. 5
- [28] Davide Morelli, Matteo Fincato, Marcella Cornia, Federico Landi, Fabio Cesari, and Rita Cucchiara. Dress code: High-resolution multi-category virtual try-on, 2022. 5, 6

- [29] Davide Morelli, Alberto Baldrati, Giuseppe Cartella, Marcella Cornia, Marco Bertini, and Rita Cucchiara. LaDIVTON: Latent Diffusion Textual-Inversion Enhanced Virtual Try-On. In *Proceedings of the ACM International Conference on Multimedia*, 2023. 2, 7
- [30] Chong Mou, Yanze Wu, Wenxu Wu, Zinan Guo, Pengze Zhang, Yufeng Cheng, Yiming Luo, Fei Ding, Shiwen Zhang, Xinghui Li, et al. Dreamo: A unified framework for image customization. *arXiv preprint arXiv:2504.16915*, 2025. 2
- [31] Haifeng Ni and Ming Xu. Itvton: Virtual try-on diffusion transformer based on integrated image and text, 2025. 2
- [32] William Peebles and Saining Xie. Scalable diffusion models with transformers. In *Proceedings of the IEEE/CVF international conference on computer vision*, pages 4195–4205, 2023. 2
- [33] Dustin Podell, Zion English, Kyle Lacey, Andreas Blattmann, Tim Dockhorn, Jonas Müller, Joe Penna, and Robin Rombach. SDXL: Improving latent diffusion models for high-resolution image synthesis. In *The Twelfth International Conference on Learning Representations*, 2024. 2
- [34] Robin Rombach, Andreas Blattmann, Dominik Lorenz, Patrick Esser, and Björn Ommer. High-resolution image synthesis with latent diffusion models, 2021. 2
- [35] Olaf Ronneberger, Philipp Fischer, and Thomas Brox. U-net: Convolutional networks for biomedical image segmentation, 2015. 2, 5
- [36] Team Seedream, :, Yunpeng Chen, Yu Gao, Lixue Gong, Meng Guo, Qiushan Guo, Zhiyao Guo, Xiaoxia Hou, Weilin Huang, Yixuan Huang, Xiaowen Jian, Huafeng Kuang, Zhichao Lai, Fanshi Li, Liang Li, Xiaochen Lian, Chao Liao, Liyang Liu, Wei Liu, Yanzuo Lu, Zhengxiong Luo, Tongtong Ou, Guang Shi, Yichun Shi, Shiqi Sun, Yu Tian, Zhi Tian, Peng Wang, Rui Wang, Xun Wang, Ye Wang, Guofeng Wu, Jie Wu, Wenxu Wu, Yonghui Wu, Xin Xia, Xuefeng Xiao, Shuang Xu, Xin Yan, Ceyuan Yang, Jianchao Yang, Zhonghua Zhai, Chenlin Zhang, Heng Zhang, Qi Zhang, Xinyu Zhang, Yuwei Zhang, Shijia Zhao, Wenliang Zhao, and Wenjia Zhu. Seedream 4.0: Toward next-generation multimodal image generation, 2025. 6, 7
- [37] Fei Shen, Xin Jiang, Xin He, Hu Ye, Cong Wang, Xiaoyu Du, Zechao Li, and Jinhui Tang. Imagdressing-v1: Customizable virtual dressing, 2024. 2
- [38] Fei Shen, Xin Jiang, Xin He, Hu Ye, Cong Wang, Xiaoyu Du, Zechao Li, and Jinhui Tang. Imagdressing-v1: Customizable virtual dressing. In *Proceedings of the AAAI Conference on Artificial Intelligence*, pages 6795–6804, 2025. 2
- [39] Jianlin Su, Yu Lu, Shengfeng Pan, Ahmed Murtadha, Bo Wen, and Yunfeng Liu. Roformer: Enhanced transformer with rotary position embedding, 2023. 5
- [40] Zhenxiong Tan, Songhua Liu, Xingyi Yang, Qiaochu Xue, and Xinchao Wang. Ominicontrol: Minimal and universal control for diffusion transformer. 2025. 2, 5
- [41] Zhenxiong Tan, Qiaochu Xue, Xingyi Yang, Songhua Liu, and Xinchao Wang. Ominicontrol2: Efficient conditioning for diffusion transformers, 2025. 4
- [42] Ashish Vaswani, Noam Shazeer, Niki Parmar, Jakob Uszkoreit, Llion Jones, Aidan N. Gomez, Lukasz Kaiser, and Illia Polosukhin. Attention is all you need, 2023. 2
- [43] Zhou Wang, A.C. Bovik, H.R. Sheikh, and E.P. Simoncelli. Image quality assessment: from error visibility to structural similarity. *IEEE Transactions on Image Processing*, 13(4): 600–612, 2004. 6
- [44] Chenfei Wu, Jiahao Li, Jingren Zhou, Junyang Lin, Kaiyuan Gao, Kun Yan, Sheng ming Yin, Shuai Bai, Xiao Xu, Yilei Chen, Yuxiang Chen, Zecheng Tang, Zekai Zhang, Zhengyi Wang, An Yang, Bowen Yu, Chen Cheng, Dayiheng Liu, Deqing Li, Hang Zhang, Hao Meng, Hu Wei, Jingyuan Ni, Kai Chen, Kuan Cao, Liang Peng, Lin Qu, Minggang Wu, Peng Wang, Shuting Yu, Tingkun Wen, Wensen Feng, Xiaoxiao Xu, Yi Wang, Yichang Zhang, Yongqiang Zhu, Yujia Wu, Yuxuan Cai, and Zenan Liu. Qwen-image technical report, 2025. 6, 7
- [45] Shaojin Wu, Mengqi Huang, Wenxu Wu, Yufeng Cheng, Fei Ding, and Qian He. Less-to-more generalization: Unlocking more controllability by in-context generation. *arXiv preprint arXiv:2504.02160*, 2025. 2
- [46] Zhenyu Xie, Zaiyu Huang, Fuwei Zhao, Haoye Dong, Michael Kampffmeyer, Xin Dong, Feida Zhu, and Xiaodan Liang. Pasta-gan++: A versatile framework for high-resolution unpaired virtual try-on, 2022. 1
- [47] Yuhao Xu, Tao Gu, Weifeng Chen, and Chengcai Chen. Oot-diffusion: Outfitting fusion based latent diffusion for controllable virtual try-on. *arXiv preprint arXiv:2403.01779*, 2024. 2, 7
- [48] Han Yang, Ruimao Zhang, Xiaobao Guo, Wei Liu, Wangmeng Zuo, and Ping Luo. Towards photo-realistic virtual try-on by adaptively generating-preserving image content. In *Proceedings of the IEEE/CVF conference on computer vision and pattern recognition*, pages 7850–7859, 2020. 1, 2
- [49] Zhendong Yang, Ailing Zeng, Chun Yuan, and Yu Li. Effective whole-body pose estimation with two-stages distillation. In *Proceedings of the IEEE/CVF International Conference on Computer Vision*, pages 4210–4220, 2023. 3
- [50] Lvmin Zhang, Anyi Rao, and Maneesh Agrawala. Adding conditional control to text-to-image diffusion models, 2023. 2
- [51] Richard Zhang, Phillip Isola, Alexei A. Efros, Eli Shechtman, and Oliver Wang. The unreasonable effectiveness of deep features as a perceptual metric, 2018. 6
- [52] Jian Zhao and Hui Zhang. Thin-plate spline motion model for image animation. In *Proceedings of the IEEE/CVF conference on computer vision and pattern recognition*, pages 3657–3666, 2022. 1
- [53] Na Zheng, Xuemeng Song, Zhaozheng Chen, Linmei Hu, Da Cao, and Liqiang Nie. Virtually trying on new clothing with arbitrary poses. In *Proceedings of the 27th ACM international conference on multimedia*, pages 266–274, 2019. 2